Chiral Nanomaterials

DOI: 10.1002/ange.201201113

Hard Templating of Nanocrystalline Titanium Dioxide with Chiral Nematic Ordering**

*Kevin E. Shopsowitz, Alexander Stahl, Wadood Y. Hamad, and Mark J. MacLachlan**

Hard templating (also called nanocasting) has emerged as a powerful method for constructing new solid-state materials with periodic order.[1–3] Although silica can be prepared with a variety of periodic structures (for example, lamellar, hexagonal, cubic) and pore sizes by aqueous sol–gel methods using a surfactant template,[4,5] this method cannot generally be applied to other materials.[6,7] This limitation stems from the fact that the required precursor for many materials either condenses too quickly, disrupts the organization of the surfactant, or is not compatible with aqueous chemistry (for example, in the preparation of metal nitrides). Sometimes these problems can be overcome by using chelating ligands or by a judicious choice of solvent and template.[8–12] On the other hand, by using porous silica as a hard template, diverse nanostructured materials may be obtained with a wide variety of compositions (carbon, polymers, noble metals, and metal oxides) after etching of the silica.[13–18] The thermal stability of silica also allows for the use of high-temperature treatments to generate highly crystalline mesoporous products that may be otherwise difficult to obtain.

The hard-templating approach has been applied to the synthesis of various novel mesoporous materials. Yue et al. recently reported the synthesis of mesoporous rutile and anatase TiO_2 using SBA-15 silica as the hard template,[19] and other hard templates have been employed in the synthesis of nanostructured titania.[20] High-surface-area nanocrystalline TiO_2 is of particular interest for applications, such as dye-sensitized solar cells,[21] photocatalysts,[22] gas sensors,[23] and batteries.[24]

The incorporation of high-surface-area anatase TiO_2 into photonic structures is a further challenge that has recently garnered attention.[25,26] By using titania in colloidal crystals and inverse opals, the high refractive index of TiO_2 ($n = 2.5$–2.9) can impart a complete photonic bandgap in these materials.

To date, the synthesis of mesoporous materials has been mainly limited to the ordered pore structures obtained from the lyotropic liquid crystalline phases of surfactants and block copolymers. We have recently developed a new class of mesoporous materials with chiral nematic pore structures templated by the lyotropic liquid-crystalline phase of nanocrystalline cellulose (NCC).[27–29] Condensation of a silica precursor ($Si(OMe)_4$ in the current study) in the presence of nanocrystalline cellulose affords a composite material in which the SiO_2 surrounds NCC with a chiral nematic organization. Upon removal of the cellulose template, a porous silicate is obtained as a free-standing film that has a long-range chiral nematic structure, resulting in photonic properties. By varying the pitch of the chiral nematic composites, mesoporous materials with tunable photonic properties are obtained.

Herein, we present the synthesis of mesoporous anatase TiO_2 using chiral nematic mesoporous silica films as a hard template. We obtain free-standing films of mesoporous titania with high specific surface areas (150–230 $m^2 g^{-1}$). Structural features of the chiral nematic silica template ranging from the mesoscopic to macroscopic size regimes are retained in the product, resulting in mesoporous TiO_2 films that reflect circularly polarized light. To the best of our knowledge, this is the first example of organizing a crystalline metal oxide into a chiral nematic structure, a method that may be useful for generating novel photonic and catalytic materials.

NCC was prepared by sulfuric acid hydrolysis of kraft softwood pulp, resulting in sulfated cellulose nanocrystals. NCC-silica composite films were prepared following a recently reported procedure (a higher concentration of NCC is used in the current study to give thicker films).[27] Briefly, an NCC suspension in water was mixed with TMOS (4 g TMOS/3 g NCC) and, after stirring at room temperature for 1 h, the mixture was poured into polystyrene Petri dishes and left to dry under ambient conditions. This gave chiral nematic NCC-silica composite films with a reflectance peak centered at about 800 nm.

NCC was initially removed from the NCC-silica composite films by calcination at 540 °C to give chiral nematic mesoporous silica films (denoted as Si-Cal) with $\lambda_{max} =$ 445 nm (Supporting Information, Figure S1 a) and a BET (Brunauer–Emmett–Teller) surface area of 650 $m^2 g^{-1}$ (Figure 1 a, Supporting Information, Table S1). The blue shift of λ_{max} upon the removal of NCC is caused by both a decrease in average refractive index and contraction of helical pitch.[27] The NCC template ranges in width from 5–15 nm (TEM; Supporting Information, Figure S2), which is larger than the pore size for Si-Cal determined by N_2 adsorption (2–10 nm; Supporting Information, Figure S3 a). It therefore appears that the contraction in helical pitch that occurs during calcination is accompanied by a contraction in pore diameter.

Cellulose is readily hydrolyzed under strongly acidic conditions. We recently showed that NCC can be removed

[*] K. E. Shopsowitz, A. Stahl, Prof. M. J. MacLachlan
Department of Chemistry, University of British Columbia
2036 Main Mall, Vancouver, BC, V6T 1Z1 (Canada)
E-mail: mmaclach@chem.ubc.ca
Dr. W. Y. Hamad
FPInnovations
3800 Wesbrook Mall, Vancouver, BC, V6S 2L9 (Canada)

[**] We thank NSERC and FPInnovations for financial support.

Supporting information for this article is available on the WWW under http://dx.doi.org/10.1002/anie.201201113.

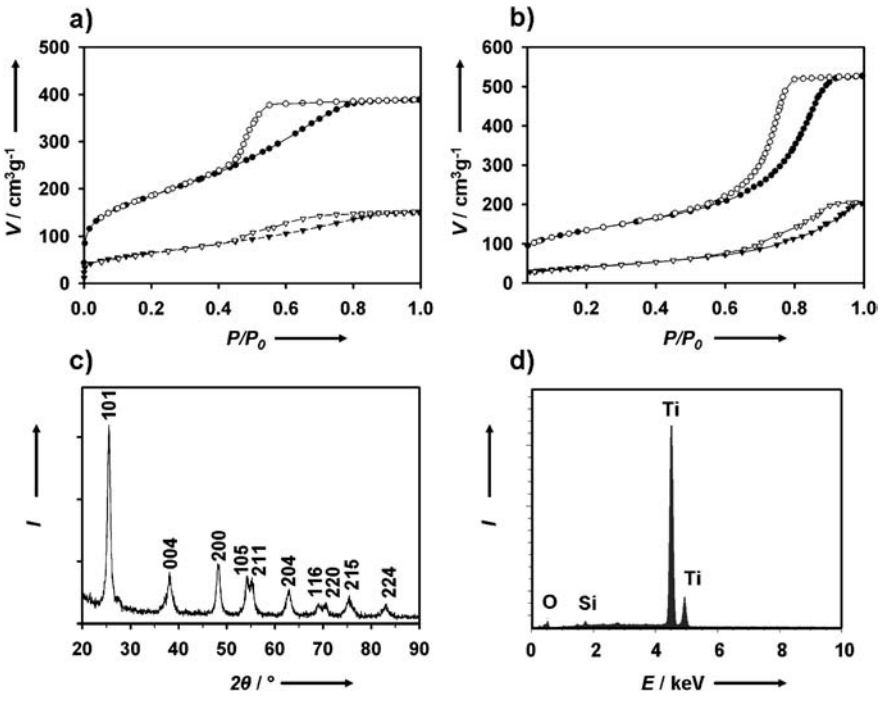

Figure 1. a,b) Nitrogen adsorption/desorption isotherms for a) Si-Cal (●,○) and Ti-Cal (▼,▽), and b) Si-Acid (●,○) and Ti-Acid (▼,▽). Filled symbols: adsorption; empty: desorption. c) Powder X-ray diffraction (PXRD) pattern for Ti-Acid. d) Energy dispersive X-ray (EDX) analysis of Ti-Acid.

from organosilica composites by acid hydrolysis, resulting in mesoporous films with larger pores (ca. 9 nm) compared to silica films prepared by calcination.[29] In the current study we used this approach to generate pure silica films with larger mesopores to use as a hard template for TiO_2 (Scheme 1) to investigate the effect of pore size on structural replication.

We tested several strong acids for removing cellulose from NCC-silica composite films and found that 12 M HCl at 85 °C causes cellulose decomposition within the films leaving behind an insoluble black residue, possibly consisting of polyfuran byproducts. Following a brief treatment of the films in strongly oxidizing conditions (5:1 H_2SO_4/H_2O_2), the black residue is removed yielding iridescent mesoporous silica films (denoted as Si-Acid). The complete removal of organic material from the silica using this procedure was confirmed by elemental analysis (% $C = 0.23$), thermogravimetric analysis (TGA), and IR spectroscopy (Supporting Information, Figure S4).

The porosity of Si-Acid was studied by N_2 adsorption, which shows a type IV isotherm and BET surface area of 471 m^2g^{-1} (Figure 1b; Supporting Information, Table S1). Si-Acid shows a substantially larger pore diameter and volume compared to Si-Cal (Supporting Information, Figure S3b, Table S1); the BJH (Barret–Joyner–Halenda model) pore size distribution for Si-Acid is fairly broad, with a peak at 10.4 nm. This distribution closely matches the range of NCC widths measured by TEM indicating that acid hydrolysis avoids the pore contraction that occurs during calcination. The mesoporous films obtained by acid hydrolysis show selective reflection centered at $\lambda_{max} = 530$ nm (Supporting Information, Figure S1b) demonstrating that the chiral nematic structure of the composite material is retained in Si-Acid. The reflectance peak of Si-Acid is red-shifted compared to Si-Cal, which further suggests that less contraction occurs during NCC removal.

Previous reports of hard templating of TiO_2 have shown that it is possible to replicate mesoscopic structures using this approach. We wanted to know whether this approach could be used to organize TiO_2 nanocrystals into a macroscopic chiral assembly by simultaneously replicating features ranging over different length scales, namely mesopores (nanometers), chiral nematic organization (micrometers), and free-standing film morphology (mm to cm).

Titania replicas were synthesized using free-standing chiral nematic mesoporous silica films with different pore sizes, Si-Acid and Si-Cal, as hard templates (denoted as Ti-Acid and Ti-Cal, respectively). The procedure employed was a variation of that reported by Yue et al.[19] An aqueous solution of $TiCl_4$ was loaded into the mesoporous silica films using the incipient wetness method. After each loading step, the films were dried and then annealed at 200 °C. After the final loading step, the silica-titania composite films were calcined at 600 °C to obtain a crystalline product. After repeating the loading four times, pore filling fractions of 75 % and 86 % were found for Si-Cal and Si-Acid, respectively (Supporting Information, Figure S5). The silica templates were then removed with 2 M $NaOH_{(aq)}$, resulting in mesoporous TiO_2. The film morphology of the mesoporous silica templates is retained in the TiO_2 replicas (Figure 2a,b), although the TiO_2 films are somewhat smaller than the original silica films. The removal of the silica template was confirmed by IR spectroscopy (Supporting Information, Figure S6) and by energy dispersive X-ray analysis (EDX;

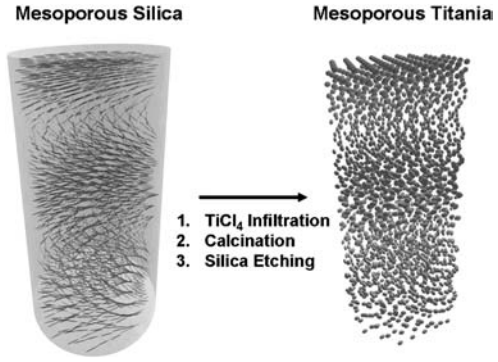

Scheme 1. Synthesis of chiral nematic titania (Ti-Cal, Ti-Acid) from chiral nematic mesoporous silica (Si-Cal, Si-Acid).

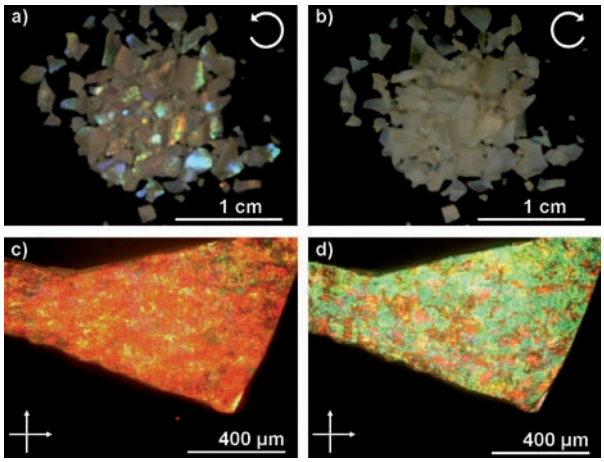

Figure 2. a) Photograph of Ti-Acid viewed under a left-handed circular polarizing filter. b) Photograph of Ti-Acid viewed under a right-handed circular polarizing filter. c) Polarized optical micrograph of a film of Ti-Acid with crossed polarizers. d) Polarized optical micrograph of Ti-Acid with crossed polarizers after the addition of ethanol.

Figure 1d). EDX analysis of the materials shows peaks corresponding to Ti, O, and a trace amount of residual Si; the Si/Ti ratio (w/w) averaged over multiple locations is about 1%. As a control, an additional sample (Ti-Control) was prepared using identical conditions in the absence of any silica hard template.

Powder X-ray diffraction (PXRD) confirms that the templated TiO_2 products, Ti-Acid and Ti-Cal, are crystalline anatase with no indication of other TiO_2 phases (Figure 1c; Supporting Information, Figure S7a). On the other hand, the TiO_2 synthesized without a template (Ti-Control) predominantly formed rutile (Supporting Information, Figure S7b). Although rutile is the most stable form of bulk TiO_2, calculations have shown that anatase becomes more stable than rutile at crystal sizes below 15 nm.[30] Thus, for Ti-Acid and Ti-Cal, nanoconfinement within the mesopores of the silica templates induces anatase to form under conditions that otherwise favor the formation of rutile.

Nitrogen adsorption measurements were performed on the TiO_2 samples (Figure 1; Supporting Information, Table S1; for the BJH pore size distributions, see Figure S3). The BET surface areas of Ti-Cal and Ti-Acid are 234 and 149 $m^2 g^{-1}$, respectively, with corresponding pore volumes of 0.23 and 0.31 $cm^3 g^{-1}$ and peak pore diameters of 2.5 and 7.9 nm. In contrast, the BET surface area of Ti-Control is only 18 $m^2 g^{-1}$, clearly demonstrating the importance of the hard template for obtaining a high-surface-area mesoporous material. It is interesting to note that the shapes of the adsorption isotherms (Figure 1) and the relative magnitudes of surface area, pore volume, and pore size for Ti-Acid and Ti-Cal reflect those of the corresponding silica templates. This demonstrates that the mesoporosity of the hard templates affects the mesoporosity of the products. The specific surface area and pore volumes of TiO_2 templated by chiral nematic mesoporous silica compares well with TiO_2 that has been templated by other mesoporous hosts.[19,20]

The hard-templated TiO_2 films are visibly iridescent (Figure 2a), thus giving a good indication that the chiral nematic structure of the mesoporous silica is retained to some degree in the TiO_2 replicas. The iridescence of the Ti-Acid films is more pronounced compared to the iridescence of the Ti-Cal films. Additionally, the Ti-Acid films are generally larger than the Ti-Cal films. These observations suggest that long-range structural replication is more effective when using Si-Acid as the template. The larger mesopores of Si-Acid may allow for more efficient diffusion and even loading of the titania precursor throughout the films, which in turn results in better long-range replication when compared to Si-Cal. The following discussion relating the optical and structural properties of the mesoporous titania and silica films is mainly limited to Ti-Acid and Si-Acid.

The iridescence of a chiral nematic structure results from the selective reflection of circularly polarized light with a handedness that matches that of the structure. The Ti-Acid films were photographed using left-handed and right-handed circular polarizing filters (LHP and RHP, respectively). The films appear strongly iridescent under an LHP filter (Figure 2a) while they simply appear white when viewed under an RHP filter (Figure 2b). This confirms the chiral nematic origin for the iridescence of the films and shows that the left-handed structure templated by NCC is preserved in the titania replicas. The iridescence of the films is still present after heating to 500 °C, demonstrating that the long-range chiral nematic structure is stable up to this temperature. However, the films lose their iridescence after heating to 900 °C, which may be due to structural rearrangement that occurs during a transition from nanocrystalline anatase to rutile (TGA of Ti-Acid suggests that this occurs around 600 °C; see the Supporting Information, Figure S8).

Scanning electron microscopy (SEM) further confirms the transfer of the chiral nematic structure from Si-Acid to Ti-Acid (Figure 3; see the Supporting Information, Figures S9, S10 for additional SEM images of Ti-Cal and Ti-Acid). A repeating helical structure is observed perpendicular to the surface of the films for both Si-Acid and Ti-Acid. One

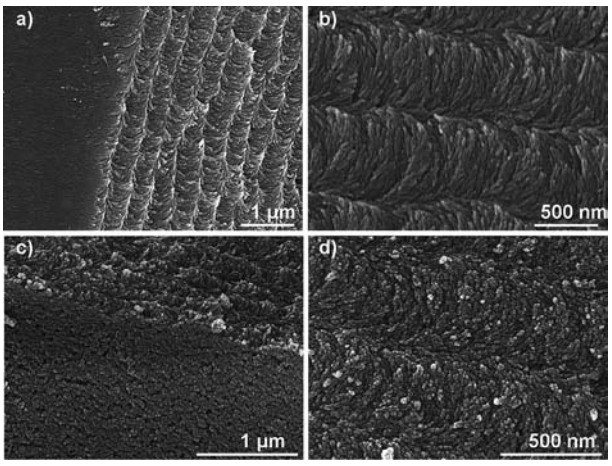

Figure 3. Scanning electron micrographs of a,b) Si-Acid and c,d) Ti-Acid. Views shown are a,c) perpendicular and b,d) parallel to the film surface.

major difference between Si-Acid and Ti-Acid is that the former is amorphous while the latter is nanocrystalline. This is clearly seen when comparing the surface of the films where the surface of Ti-Acid appears much rougher owing to the nanocrystalline morphology. The crystallization of TiO_2 drives the formation of more globular particles compared to the rod morphology of Si-Acid and the original NCC template. Thus, the helical pitch of Ti-Acid appears less ordered when compared to Si-Acid. We also observe a TiO_2 "crust" coating some of the TiO_2 films, which is most likely due to some of the $TiCl_4$ solution condensing on the surface of the films as opposed to within the mesopores (Supporting Information, Figure S10 d). This is due to the imperfect loading achieved using the incipient wetness technique and could likely be overcome by using an alternative technique such as atomic layer deposition.

Looking at Ti-Acid using polarized optical microscopy (POM), the films are strongly birefringent, further confirming the long-range anisotropy of the materials (Figure 2 c). Upon addition of ethanol, the films remain birefringent, but POM shows a large change in coloration (Figure 2 d). This change is reversible, and the films regain their original color when the ethanol has evaporated. This marked change in birefringence gives clear evidence that the pores of the mesoporous TiO_2 are accessible to guest molecules and that pore infiltration can cause a change in optical properties. The change in birefringence upon solvent loading of the TiO_2 films is markedly different than for the SiO_2 films. When isotropic liquids (for example, water or ethanol) are added to Si-Acid or Si-Cal, the iridescence and birefringence of the films are almost completely shut off.[27] We have attributed this effect to refractive index matching, as the refractive index of SiO_2 closely matches those of the isotropic liquids that were investigated. The refractive index of TiO_2, however, is much higher than that of SiO_2. We therefore expect to see a smaller change in the optical properties of the TiO_2 films upon soaking with isotropic liquids. These findings demonstrate that the optical response of porous chiral nematic materials can be tailored by changing the optical properties of the "walls".

To summarize, we have shown, for the first time, that chiral nematic mesoporous silica can be used as a template to synthesize titania. In this hard-templating method, structural features are replicated at several length scales: 1) the titania is mesoporous with a surface area and pore size that is determined by the porosity of the starting silica template; 2) the material obtained selectively reflects left-handed circularly polarized light, which indicates a chiral nematic organization of the titania crystallites; and 3) the titania is obtained as films with similar dimensions as the original silica films. These novel highly porous films of titania may be excellent materials for applications in dye-sensitized solar cells, photocatalysts, sensors, and batteries. Using this hard-templating method, we expect that other mesoporous metal oxide structures with chiral nematic organization may be prepared.

Experimental Section

The preparation of NCC-silica composite films and Si-Cal has been reported previously.[27] See the Supporting Information for the exact procedure used herein and for the preparation of Si-Acid.

TiO_2 replica films: A freshly prepared $TiCl_4$ solution (ca. 4.3 M) was added to the mesoporous silica using the incipient wetness method. A volume of $TiCl_4$ solution equivalent to the pore volume of mesoporous silica that was used was added to the silica films. For example, Ti-Acid was prepared by adding 105 μL of $TiCl_4$ solution to 130 mg of Si-Acid (pore volume of Si-Acid: 0.81 $cm^3 g^{-1}$). The $TiCl_4$ loaded films were then dried at 80 °C for 30 min before heating to 200 °C for 1 h under air to induce TiO_2 formation. This procedure was repeated four times in total to ensure sufficient pore loading of the films. After the final loading step, the TiO_2/SiO_2 films were calcined at 600 °C to facilitate TiO_2 crystallization giving 202 mg of TiO_2/SiO_2 composite films. The composite films were then placed in a 2 M NaOH solution for 18 h at 20 °C to selectively remove the silica. The resulting TiO_2 films were then recovered by filtration, washed with copious amounts of water, and allowed to air dry giving 117 mg of Ti-Acid. Ti-Cal was prepared by an analogous procedure. Ti-Control was prepared by the same procedure in a vial that did not contain any mesoporous silica template.

Received: February 9, 2012
Published online: May 25, 2012

Keywords: chirality · hard templating · mesoporous materials · nanocrystalline cellulose · titanium dioxide

[1] a) A. Lu, F. Schüth, *Adv. Mater.* **2006**, *18*, 1793 – 1805; b) H. Yang, D. Zhao, *J. Mater. Chem.* **2005**, *15*, 1217 – 1231; c) R. A. Caruso, *Top. Curr. Chem.* **2003**, *226*, 91 – 118.
[2] a) R. Ryoo, S. H. Joo, S. Jun, *J. Phys. Chem. B* **1999**, *103*, 7743 – 7746; b) J. Lee, S. Yoon, T. Hyeon, S. M. Oh, K. B. Kim, *Chem. Commun.* **1999**, 2177 – 2178.
[3] For recent examples, see: a) H. Liu, G. Wang, J. Liu, S. Qiao, H. Ahn, *J. Mater. Chem.* **2011**, *21*, 3046 – 3052; b) W.-C. Li, G.-Z. Nong, A.-H. Lu, H.-Q. Hu, *J. Porous Mater.* **2011**, *18*, 23 – 30; c) G. S. Armatas, A. P. Katsoulidis, D. E. Petrakis, P. J. Pomonis, M. G. Kanatzidis, *Chem. Mater.* **2010**, *22*, 5739 – 5746; d) T. Waitz, B. Becker, T. Wagner, T. Sauerwald, C.-D. Kohl, M. Tiemann, *Sens. Actuators B* **2010**, *150*, 788 – 793; e) T. Garcia, S. Agouram, J. F. Sanchez-Royo, R. Murillo, A. M. Mastral, A. Aranda, I. Vazquez, A. Dejoz, B. Solsona, *Appl. Catal. A* **2010**, *386*, 16 – 27.
[4] C. T. Kresge, M. E. Leonowicz, W. J. Roth, J. C. Vartuli, J. S. Beck, *Nature* **1992**, *359*, 710 – 712.
[5] Y. Wan, D. Zhao, *Chem. Rev.* **2007**, *107*, 2821 – 2860.
[6] M. G. Kanatzidis, *Adv. Mater.* **2007**, *19*, 1165 – 1181.
[7] For examples of exceptions, see: a) M. J. MacLachlan, N. Coombs, G. A. Ozin, *Nature* **1999**, *397*, 681 – 684; b) M. Fröba, N. Oberender, *Chem. Commun.* **1997**, 1729 – 1730; c) C. D. Liang, K. L. Hong, G. A. Guiochon, J. W. Mays, S. Dai, *Angew. Chem.* **2004**, *116*, 5909 – 5913; *Angew. Chem. Int. Ed.* **2004**, *43*, 5785 – 5789.
[8] H. Qi, X. Roy, K. E. Shopsowitz, J. K.-H. Hui, M. J. MacLachlan, *Angew. Chem.* **2010**, *122*, 9934 – 9937; *Angew. Chem. Int. Ed.* **2010**, *49*, 9740 – 9743.
[9] D. Sun, A. E. Riley, A. J. Cadby, E. K. Richman, S. D. Korlann, S. H. Tolbert, *Nature* **2006**, *441*, 1126 – 1130.
[10] a) P. N. Trikalitis, K. K. Rangan, T. Bakas, M. G. Kanatzidis, *Nature* **2001**, *410*, 671 – 675; b) R. W. J. Scott, N. Coombs, G. A. Ozin, *J. Mater. Chem.* **2003**, *13*, 969 – 974.
[11] Y. Yamauchi, K. Kuroda, *Chem. Asian J.* **2008**, *3*, 664 – 676.

[12] a) X. Roy, L. K. Thompson, N. Coombs, M. J. MacLachlan, *Angew. Chem.* **2008**, *120*, 521 – 524; *Angew. Chem. Int. Ed.* **2008**, *47*, 511 – 514; b) F. Sediri, M. K. Chine, N. Gharbi, *Opt. Mater.* **2008**, *30*, 1521 – 1526.
[13] For a recent review of mesoporous carbon materials, see: C. Liang, Z. Li, S. Dai, *Angew. Chem.* **2008**, *120*, 3754 – 3776; *Angew. Chem. Int. Ed.* **2008**, *47*, 3696 – 3717.
[14] For a recent review of hard-templated polymers, see: A. Thomas, F. Goettmann, M. Antonietti, *Chem. Mater.* **2008**, *20*, 738 – 755.
[15] Y. J. Han, J. M. Kim, G. D. Stucky, *Chem. Mater.* **2000**, *12*, 2068 – 2069.
[16] Z. Liu, Y. Sakamoto, T. Ohsuna, K. Hiraga, O. Terasaki, C. H. Ko, H. J. Shin, R. Ryoo, *Angew. Chem.* **2000**, *112*, 3237 – 3240; *Angew. Chem. Int. Ed.* **2000**, *39*, 3107 – 3110.
[17] B. Tian, X. Liu, L. A. Solovyov, Z. Liu, H. Yang, Z. Zhang, S. Xie, F. Zhang, B. Tu, C. Yu, O. Terasaki, D. Zhao, *J. Am. Chem. Soc.* **2004**, *126*, 865 – 875.
[18] B. Tian, X. Liu, H. Yang, S. Xie, C. Yu, B. Tu, D. Zhao, *Adv. Mater.* **2003**, *15*, 1370 – 1374.
[19] a) W. Yue, X. Xu, J. T. S. Irvine, P. S. Attidekou, C. Liu, H. He, D. Zhao, W. Zhou, *Chem. Mater.* **2009**, *21*, 2540 – 2546; b) W. Yue, C. Randorn, P. S. Attidekou, Z. Su, J. T. S. Irvine, W. Zhou, *Adv. Funct. Mater.* **2009**, *19*, 2826 – 2833.
[20] a) W.-S. Chae, S.-W. Lee, Y.-R. Kim, *Chem. Mater.* **2005**, *17*, 3072 – 3074; b) Y. Xia, R. Mokaya, *J. Mater. Chem.* **2005**, *15*, 3126 – 3131; c) J. C. Lytle, H. Yan, R. T. Turgeon, A. Stein, *Chem. Mater.* **2004**, *16*, 3829 – 3837.
[21] B. O'Regan, M. Grätzel, *Nature* **1991**, *353*, 737 – 740.
[22] a) S. Zhang, D. Jiang, T. Tang, J. Li, Y. Xu, W. Shen, J. Xu, F. Deng, *Catal. Today* **2010**, *158*, 329 – 335; b) C. Aprile, A. Corma, H. Garcia, *Phys. Chem. Chem. Phys.* **2008**, *10*, 769 – 783.
[23] a) V. Guidi, M. C. Carotta, M. Ferroni, G. Martinelli, L. Paglialonga, E. Comini, G. Sberveglieri, *Sens. Actuators B* **1999**, *57*, 197 – 200; b) C. Wang, L. Yin, L. Zhang, Y. Qi, N. Lun, N. Liu, *Langmuir* **2010**, *26*, 12841 – 12848.
[24] a) S. Y. Huang, L. Kavan, I. Exnar, M. Gratzel, *J. Electrochem. Soc.* **1995**, *142*, L142 – L144; b) M. Wagemaker, A. P. M. Kentgens, F. M. Mulder, *Nature* **2002**, *418*, 397 – 399.
[25] J. E. G. J. Wijnhoven, W. L. Vos, *Science* **1998**, *281*, 802 – 804.
[26] a) R. C. Schroden, M. Al-Daous, C. F. Blanford, A. Stein, *Chem. Mater.* **2002**, *14*, 3305 – 3315; b) Y. Xu, X. Zhu, Y. Dan, J. H. Moon, V. W. Chen, A. T. Johnson, J. W. Perry, S. Yang, *Chem. Mater.* **2008**, *20*, 1816 – 1823; c) J. I. L. Chen, G. von Freymann, S. Y. Choi, V. Kitaev, G. A. Ozin, *Adv. Mater.* **2006**, *18*, 1915 – 1919.
[27] K. E. Shopsowitz, H. Qi, W. Y. Hamad, M. J. MacLachlan, *Nature* **2010**, *468*, 422 – 425.
[28] K. E. Shopsowitz, W. Y. Hamad, M. J. MacLachlan, *Angew. Chem.* **2011**, *123*, 11183 – 11187; *Angew. Chem. Int. Ed.* **2011**, *50*, 10991 – 10995.
[29] K. E. Shopsowitz, W. Y. Hamad, M. J. MacLachlan, *J. Am. Chem. Soc.* **2012**, *134*, 867 – 870.
[30] H. Zhang, J. F. Banfield, *J. Mater. Chem.* **1998**, *8*, 2073 – 2076.

